ARTICLE

Mutations in a BTB-Kelch Protein, KLHL7, Cause Autosomal-Dominant Retinitis Pigmentosa

James S. Friedman,[1] Joseph W. Ray,[2] Naushin Waseem,[3] Kory Johnson,[4] Matthew J. Brooks,[1] Therése Hugosson,[5] Debra Breuer,[6] Kari E. Branham,[6] Daniel S. Krauth,[1] Sara J. Bowne,[2] Lori S. Sullivan,[2] Vesna Ponjavic,[5] Lotta Gränse,[5] Ritu Khanna,[6] Edward H. Trager,[6] Linn M. Gieser,[1] Dianna Hughbanks-Wheaton,[7] Radu I. Cojocaru,[1] Noor M. Ghiasvand,[6,12] Christina F. Chakarova,[3] Magnus Abrahamson,[8] Harald H.H. Göring,[9] Andrew R. Webster,[3] David G. Birch,[7] Goncalo R. Abecasis,[10] Yang Fann,[4] Shomi S. Bhattacharya,[3] Stephen P. Daiger,[2] John R. Heckenlively,[6] Sten Andréasson,[5] and Anand Swaroop[1,6,11,*]

Retinitis pigmentosa (RP) refers to a genetically heterogeneous group of progressive neurodegenerative diseases that result in dysfunction and/or death of rod and cone photoreceptors in the retina. So far, 18 genes have been identified for autosomal-dominant (ad) RP. Here, we describe an adRP locus (RP42) at chromosome 7p15 through linkage analysis in a six-generation Scandinavian family and identify a disease-causing mutation, c.449G→A (p.S150N), in exon 6 of the *KLHL7* gene. Mutation screening of *KLHL7* in 502 retinopathy probands has revealed three different missense mutations in six independent families. *KLHL7* is widely expressed, including expression in rod photoreceptors, and encodes a 75 kDa protein of the BTB-Kelch subfamily within the BTB superfamily. BTB-Kelch proteins have been implicated in ubiquitination through Cullin E3 ligases. Notably, all three putative disease-causing KLHL7 mutations are within a conserved BACK domain; homology modeling suggests that mutant amino acid side chains can potentially fill the cleft between two helices, thereby affecting the ubiquitination complexes. Mutations in an identical region of another BTB-Kelch protein, gigaxonin, have previously been associated with giant axonal neuropathy. Our studies suggest an additional role of the ubiquitin-proteasome protein-degradation pathway in maintaining neuronal health and in disease.

Introduction

Retinal diseases are a major cause of inherited irreversible vision loss worldwide. Retinitis pigmentosa (RP [MIM 268000]) refers to a clinically diverse group of retinal degenerative diseases that are characterized by night blindness, bone spicule-like pigmentation, and progressive constriction of visual fields.[1] Degeneration of rod and cone photoreceptors constitutes the major pathological manifestation of RP, which may be inherited in an autosomal-dominant (ad), autosomal-recessive, or X-linked manner.[1,2] To date, 192 retinal disease loci have been mapped and 144 genes identified (see RetNet website). Mutations in at least 60 genes may cause RP; of these, 18 genes have been associated with ad forms of RP. Screening of the 18 disease genes has led to detection of mutations in 50%–60% of adRP families; thus, genetic defects in many patients are yet to be identified.[3]

The adRP genes encode an array of proteins involved in diverse biological functions, including phototransduction, gene regulation, splicing, and photoreceptor outer segment morphogenesis.[1,2] Notably, a vast majority of adRP proteins are widely expressed, yet most genetic defects specifically lead to photoreceptor degeneration. Multiple causes of photoreceptor dysfunction or death have been proposed. These include improper levels of cyclic nucleotides, calcium ion influx, and oxidative stress.[4] However, the molecular etiology and biochemical mechanism(s) of most forms of adRP still remain to be elucidated.

We describe here the mapping of an adRP locus (RP42) by whole-genome scan of a large Scandinavian family and identify the disease-causing mutation in a BTB-Kelch protein, *KLHL7* (MIM 611119). Additional screening of 502 retinopathy patients from North America and Europe has revealed a total of three missense mutations in *KLHL7* in six families. The three mutations appear to affect the predicted KLHL7 protein structure, as indicated by in silico homology modeling. On the basis of the presence of BTB and Kelch domains, we suggest that KLHL7 participates as an adaptor and/or chaperone in the ubiquitin-proteasome protein-degradation pathway.

[1]Neurobiology-Neurodegeneration & Repair Laboratory (N-NRL), National Eye Institute, National Institutes of Health (NIH), Bethesda, MD 20892, USA; [2]Human Genetic Center, The University of Texas Health Science Center, Houston, TX 77030, USA; [3]Department of Molecular Genetics, Institute of Ophthalmology, London, EC1 9EL, UK; [4]Bioinformatics Section, Division of Intramural Research, National Institute of Neurological Disorders and Stroke, NIH, Bethesda, MD 20892, USA; [5]Department of Ophthalmology, Lund University Hospital, S-221 85 Lund, Sweden; [6]Department of Ophthalmology, University of Michigan, Ann Arbor, MI 48105, USA; [7]Retina Foundation of the Southwest, Dallas, TX 75231, USA; [8]Department of Laboratory Medicine, Lund University, S-221 85 Lund, Sweden; [9]Department of Genetics, Southwest Foundation for Biomedical Research, San Antonio, TX 78227, USA; [10]Center for Statistical Genetics, Department of Biostatistics, University of Michigan, Ann Arbor, MI 48105, USA; [11]Department of Human Genetics, University of Michigan Medical School, Ann Arbor, MI 48109, USA
[12]Present address: Department of Biology, Grand Valley State University, Allendale, MI 49401, USA
*Correspondence: swaroopa@mail.nih.gov
DOI 10.1016/j.ajhg.2009.05.007.

Subjects and Methods

Genotyping and Linkage Analysis

Human studies were approved by their respective institutional review boards and performed in accordance with the Declaration of Helsinki. DNA samples from 23 individuals of Scandinavian adRP family 72 were hybridized to Affymetrix SNP Nsp 250K array according to the manufacturer's recommendations (Affymetrix, Santa Clara, CA, USA). After scanning, the CEL files were analyzed with the BRLMM Analysis Tool 1.0 (Affymetrix). The resulting brlmm file was imported into Alohomora[5] and analyzed with GRR[6] and Pedstats[7] for a check of the integrity of the pedigree and selection of uninformative and/or mistyped SNPs for removal from the data set. SNPs were subsequently exported into Mega2[8] and reformatted as individual chromosomes for linkage in Merlin.[9] Multipoint linkage analysis was performed with a parametric model assuming an ad mode of inheritance, a disease-allele frequency of 0.0001, and 100% penetrance.

Human-Mutation Screen

We carried out a mutation screen of *KLHL7* in patients or controls collected from North America (Michigan and Texas cohorts), Scandinavia, and the UK. The North American retinopathy cohort collected in Michigan has been previously described.[10] Of the 282 patients screened in this cohort, 170 have RP and nine are known to have adRP. PCR primer sets are listed in Table S1 (available online). PCR amplified DNA was sequenced using ABI 3130xl Genetic Analyzer (Applied BioSystems, Foster City, CA).

RT-PCR

RNA samples from mouse tissues and flow sorted GFP-tagged photoreceptors were used as templates for RT-PCR. The *KLHL7* PCR primers spanned an intron. The primers are listed in Table S2.

Immunoblot Analysis

Procedures with mice were followed in accordance with the ethical standards of the National Eye Institute (NEI) Animal Care and Use Committee at NIH. Retinas from C57BL/6J mice were sonicated in PBS and 3X protease inhibitor cocktail (Roche, Indianapolis, IN, USA) and centrifuged at 16,000 × *g* for 5 min at 4°C. The protein extract was analyzed with NuPAGE 10% bis-Tris gel (Invitrogen, Carlsbad, CA, USA). Proteins were transferred to Hybond membrane (Amersham Biosciences, Piscataway, NJ, USA) in NuPAGE transfer buffer (Invitrogen). The membrane was preincubated in 5% nonfat milk in TBS with 0.1% Tween 20 (TBST) for 1 hr at room temperature and then incubated with a mouse α-KLHL7 polyclonal antibody (Abnova, Walnut, CA, USA; 1:2000, stored in 50% glycerol) overnight at 4°C. After washing, the blot was incubated with a donkey α-mouse HRP (Jackson Immunoresearch, West Grove, PA, USA; 1:4000) secondary antibody in 5% TBST, washed again, and visualized via chemiluminescence (Thermoscientific, Rockford, IL, USA).

Immunostaining

Cryosectioned slides of C57BL/6J mouse retinas (10 μm) were preincubated with 5% BSA diluted in PBS containing 0.2% Tween 20 (PBST) for 30 min at room temperature. Sections were then incubated with a mouse α-KLHL7 polyclonal antibody (Abnova; 1:400), in 2% BSA diluted in PBST, overnight at 4°C in a humidity chamber. After three rinsings with PBST, sections were incubated with a goat α-mouse Alexafluor 488 secondary antibody (Invitrogen; 1:1000), in 2% BSA diluted in PBST, for 30 min at room temperature in a humidification chamber. Sections were then stained with DAPI (Invitrogen; 1:1000) for 2 min, rinsed three times with PBST, and mounted with gel mount (Electron Microscopy Sciences, Hatfield, PA, USA). Confocal microscopy of immunostained sections was carried out on a Leica confocal microscope. Leica software was used for imaging and analysis.

Retinas from the adult Nrl-p-GFP mice[11] were dissected in DMEM medium (Invitrogen), cut into small pieces, and dissociated by continuous mixing in DMEM medium, containing Papain at a concentration of 8.5 U per mL (Sigma, St. Louis, MO, USA) and 0.29 mM L-cysteine (Sigma), at 37°C for 15 min. Dissociated cells (including photoreceptors) were fixed for 10 min at room temperature, then for 20 min at 37°C in 4% paraformaldehyde in PBS. Immunostaining was carried out as described above.

Protein Structure Modeling and Residue Permutation

Homology modeling was accomplished with the use of SWISS-MODEL in automated mode.[12–15] The protein sequence used (NP_001026880.2) was obtained via NCBI-Entrez. Residue permutation was carried out with WHAT IF.[16] Energy minimization, superposition, and root-mean-square deviation (RMSD) calculations were performed in DeepView (v4.0.1). Finished structures were rendered in POV-Ray.

Results

Mapping of a New adRP Locus RP42 to Chromosome 7p15

We have been studying a large six-generation Scandinavian family (family 72)[17] afflicted with a slow progressing retinopathy (Figure 1A). The retinal fundus image and full-field electroretinogram (ERG) of the proband V.8 (Figures 1B and 1C) demonstrate a late-onset RP with mild and slower than usual progression of disease. Similar findings were observed in other family members, though some had a more aggressive form of retinal degeneration. Given that analysis of polymorphic markers excluded the involvement of previously mapped adRP loci (data not shown), we undertook a whole-genome scan of 23 individuals in family 72 with the use of Affymetrix Nsp 250K SNP chips. Linkage analysis of genotyping data via Merlin[9] revealed a multipoint peak LOD score of 5.0 on chromosome 7p15 for this adRP locus (called RP42) (Figure 1D). The results of the whole-genome linkage scan are shown in Figure S1.

Identification of a Missense Mutation in KLHL7

Evaluation of haplotypes in family 72 determined an approximately 3 Mb critical region, flanked by markers SNP_A-4196981 (rs4719697) and SNP_A-1989250 (rs2188993). This critical region included 30 annotated or predicted genes (Figures 1E and 1F). The RP42 locus is distinct from the previously reported RP9 locus (MIM 607331), which is flanked by markers D7S526 and D7S484.[18] An ad cystoid macular dystrophy locus (CYMD [MIM 153880]), previously mapped to a 20 cM region flanked by markers D7S493 and D7S526,[19] overlaps

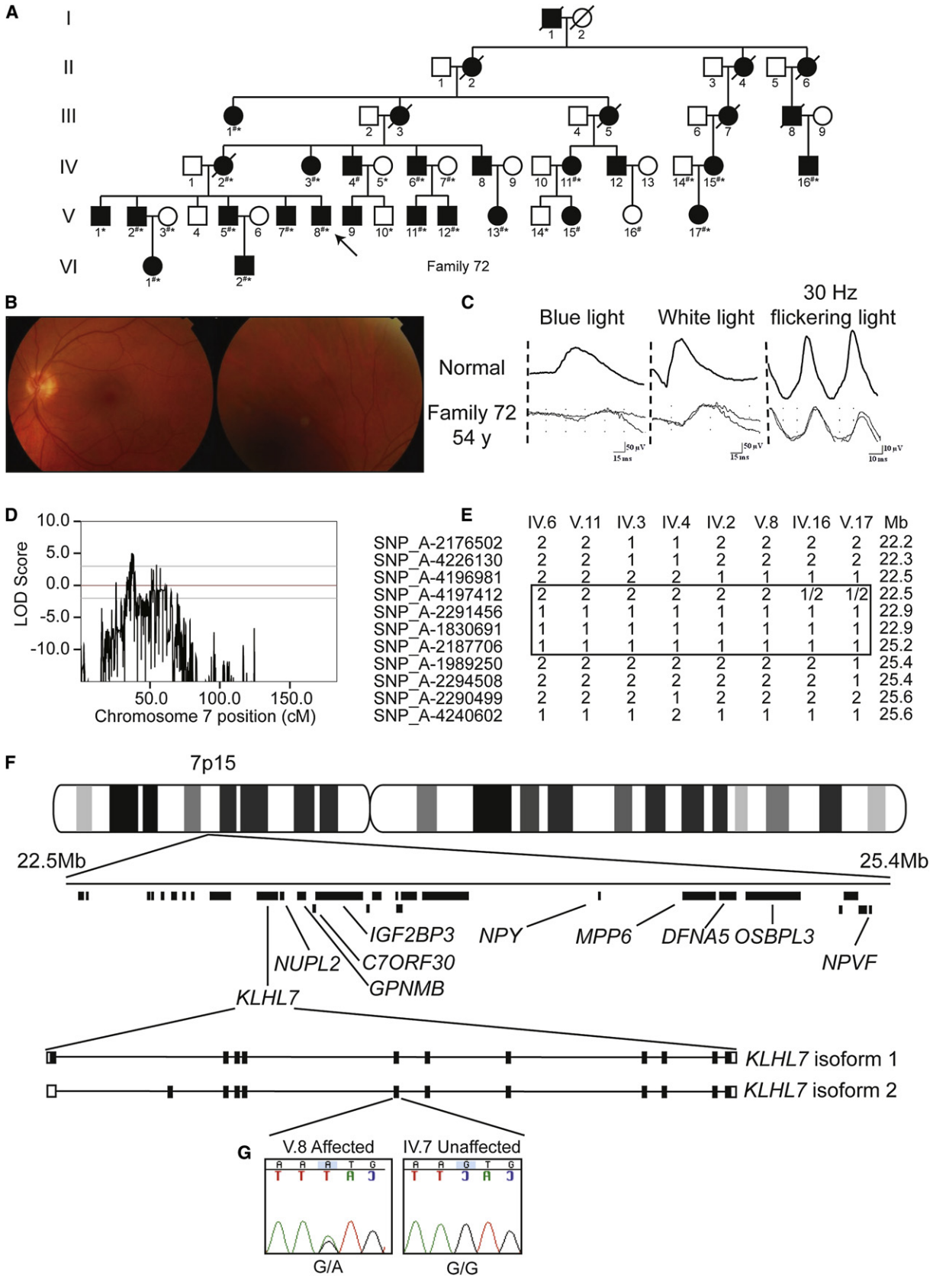

Figure 1. Linkage Analysis and Genetic Screen of Family 72

(A) Pedigree of family 72. Individuals genotyped for linkage are noted by number symbols. Individuals sequenced in exon 6 of *KLHL7* are noted with an asterisk.

with the RP42 locus. We performed mutation screens of several genes within the RP42 critical interval by sequencing predicted or known exons and corresponding exon-intron boundary regions. No obvious disease-causing variants were detected in *NUPL2*, *GPNMB* (MIM 604368), *C7ORF30*, *IGF2BP3* (MIM 608259), *NPY* (MIM 162640), *MPP6* (MIM 606959), *DFNA5* (MIM 608798), *OSBPL3* (MIM 606732), or *NPVF*. We subsequently discovered a nonsynonymous and potentially disease-causing c.449G→A, p.S150N mutation in exon 6 of the *KLHL7* gene (Figure 1G). This change segregated perfectly with the disease in 24 family members that were examined. Evaluation of 102, 183, and 185 unaffected control individuals from Scandinavia, North America, and the UK, respectively, did not reveal an S150N variant.

KLHL7 Mutation Screening in Retinopathy Patients

We then screened the *KLHL7* gene for possible mutations in 502 unrelated adRP probands from Europe and North America (Figure 2). The c.449G→A, p.S150N sequence alteration, detected in Scandinavian family 72, was also discovered in two affected individuals of an RP family from North America (RFS073). Another independent putative mutation, c.458C→T, p.A153V, was observed in three families. This variant was concordant in 11 members of Scandinavian family 101, detected in the proband of UK family RP9713, and identified in three affected individuals of North American family RFS038 (Figure 2). A third independent and potentially disease-causing change at residue c.457G→A, encoding a p.A153T alteration, was uncovered in a patient from North American family RFS061 (Figure 2H). However, other members of this family were unavailable for genetic analysis. Additional genetic variants of uncertain significance are summarized in Table 1.

To test the likelihood that the *KLHL7* mutations (reported here) cause disease, we performed an additional linkage experiment combining families 101, RFS073, and RFS038, grouping the mutant allele from each family as a single marker. Our analysis generated a LOD score of 3.185, indicating that the observed genotype is 1530 times more likely to occur when the gene is completely linked to the trait. This analysis further supports the likelihood that mutations in *KLHL7* cause disease.

All three missense mutations that we report here in six independent adRP families are present in exon 6 of *KLHL7* and were not observed in 470 controls from North America, Scandinavia, or the UK. Both S150 and A153 residues are completely conserved in 12 orthologs of KLHL7 from human to fugu. Of the 38 currently annotated human "Kelch-like" proteins in the NCBI database, neither amino acid residue is completely conserved through evolution. However, we speculate that the secondary structure of this region of the BACK domain is conserved.

We also observed two individuals with putative disease-causing mutations, c.763G→A (p.D255N) and c.1414A→G (p.K472Q). Although these changes were not present in 166 controls, we were not able to test segregation of these alterations with disease. Until functional effect of these changes is demonstrated, we consider D255N and K472Q to be of uncertain significance.

Overall, on the basis of analysis of a cohort previously used for ascertaining prevalence of adRP mutations,[3] we estimate that *KLHL7* is responsible for 1%–2% of adRP.

Expression Profile of KLHL7

RT-PCR analysis revealed that *Klhl7* is widely expressed in mouse tissues (Figure 3A). Immunoblot analysis of retinal extracts with the use of a commercial α-KLHL7 antibody showed a single, somewhat larger than predicted protein band of 75 kDa (Figure 3B). It is therefore likely that KLHL7 is subject to posttranslational modifications. Immunohistochemical analysis demonstrated cytoplasmic staining with some perinuclear distribution of KLHL7 in ganglion cell and inner nuclear layers of adult mouse retina (Figure 3C). A pattern that was similar but with lower intensity was detected in photoreceptors. RT-PCR and immunocytochemistry experiments of GFP-tagged rods enriched from the retina of *Nrl*-GFP mice,[11] together with in silico analysis of microarray data,[11] validated the expression of KLHL7 in rod photoreceptors (Figures 3A and 3D).

Analysis of the KLHL7 Protein Structure

KLHL7 encodes two transcripts with distinct 5′- exons (Figure 1F), thereby coding for predicted protein isoforms of 564 and 586 residues with different N-terminal regions. (Figure 4A shows KLHL7 isoform 1 with putative mutations.) Both isoforms of KLHL7 contain BTB (Bric-a-brac,

(B) Fundus photograph of individual V.8. Very mild degeneration is observed.
(C) ERG traces of individual V.8 illustrate isolated rod responses to single flashes of blue light (left column), mixed responses to single flashes of white light (middle column), and isolated cone responses to 30 Hz flickering light (right column).
(D) Linkage analysis of 23 individuals from family 72. A peak multipoint LOD score of 5.0 was obtained on chromosome 7p15.
(E) Disease-chromosome haplotypes of individuals IV.6, V.11, IV.3, IV.4, IV.2, V.8, IV.16, and V.17. Recombinations between SNP_A-4196981 (rs4719697) and SNP_A-4197412 (rs3857716), and SNP_A-2187706 (rs7780038) and SNP_A-1989250 (rs2188993), respectively, denote the critical region. Mb denotes Megabase.
(F) Physical map of the adRP critical region. Mb denotes Megabase. Genes completely screened for mutations are labeled. The intron-exon structure for *KLHL7* isoforms 1 and 2 are shown.
(G) Chromatogram of *KLHL7* exon 6 sequences in individuals V.8 and IV.7 from family 72 are shown. Proband V.8 contains a heterozygous G-to-A transition, c.449G→A, leading to a predicted p.S150N amino acid change. A related unaffected individual, IV.7, has a homozygous G at the same residue.

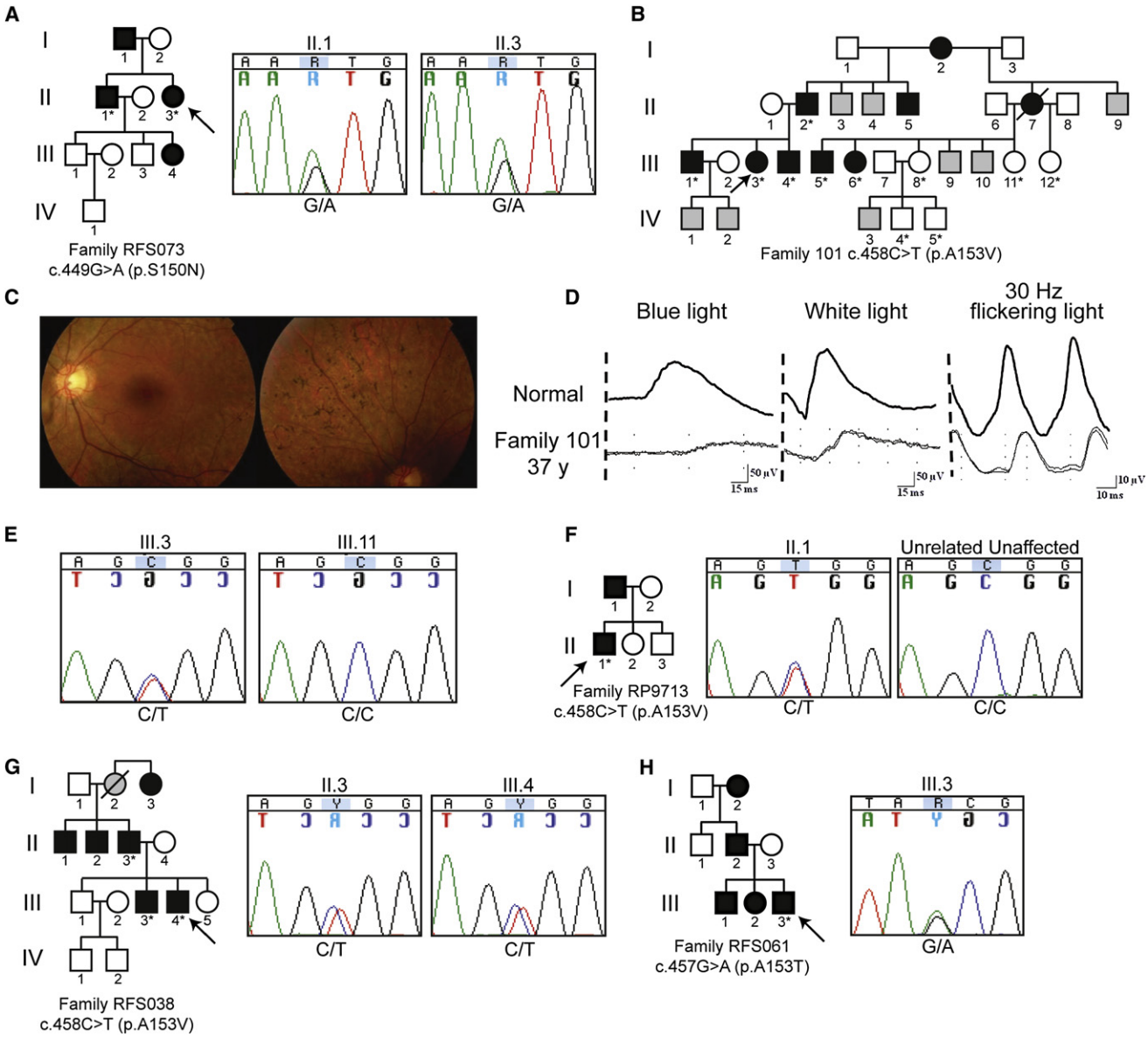

Figure 2. Mutation Screen of *KLHL7*

Individuals in pedigrees sequenced in exon 6 of *KLHL7* are denoted with an asterisk. Probands are marked with an arrow. Individuals of unknown phenotype are marked with gray.

(A) Pedigree and chromatograms of a c.449G→A-containing proband in North American family RFS073. Sequences of II.1 and II.3 are shown.

(B) Pedigree of Scandinavian adRP family 101.

(C) Fundus photograph of individual III.3. Retinal degeneration and pigmentation are observed.

(D) ERG analysis of individual III.3. Rod and cone photoreceptor responses were moderately reduced.

(E) Chromatograms of individuals III.3 and III.11, showing the c.458C→T mutation and no change, respectively.

(F) Pedigree of UK family RP9713. Chromatogram of individual II.1, with the c.458C→T change, and an unrelated unaffected individual.

(G) Pedigree of North American adRP family RFS038. Chromatograms of individuals II.3, III.3, and III.4 reveal the c.458C→T mutation.

(H) Pedigree of North American adRP family RFS061. Chromatogram of proband III.3, showing the c.457G→A mutation.

Tramtrack, and Broad Complex), BACK, and Kelch functional domains, suggesting that KLHL7 is a BTB-Kelch protein.[20,21] Homology modeling of the three KLHL7 domains shows respective similarity to (1) the BTB domain of B cell lymphoma 6 (BCL6 [PDB: 1r29A]), (2) the BACK domain of Kbtbd4 (PDB: 2eqxA), and (3) the Kelch domain of KLHL12 (PDB: 2vpjA). All three mutations that we identified are within the alpha helical secondary structure α1 of the KLHL7 homology model, ascertained on the basis of the solution structure of Kbtbd4 (PDB: 2eqxA) (Figure 4B). Tertiary models of each mutation in the KLHL7 homology model revealed only a subtle effect on

Table 1. A Summary of the *KLHL7* Mutation Screen in Retinopathy Patients

		Scandinavia adRP Cohort		United Kingdom adRP Cohort		University of Michigan N.A. Retinopathy Cohort		University of Texas N.A. adRP Cohort		
		Proband	Control	Proband	Control	Proband	Control	Proband	Control	DB SNP ID
Putative Disease-Causing Changes										
Exon 6	c.449G→A (p.S150N)	1	0	0	0	0	0	1	N/A	
Exon 6	c.457G→A (p.A153T)	0	0	0	0	0	0	1	N/A	
Exon 6	c.458C→T (p.A153V)	1	0	1	0	0	0	1	N/A	
Variants										
5′ UTR	c.-235G→T	N/A	N/A	0	N/A	3	N/A	N/A	N/A	
5′ UTR	c.-118G→A	N/A	N/A	0	N/A	1	N/A	N/A	N/A	
Exon 2	c.53A→G (p.K18R, isoform 2)	N/A	N/A	0	N/A	4	N/A	1	N/A	rs17147682
Exon 5	c.352C→T (p.L118L)	N/A	N/A	0.64 C, 0.36 T	N/A	0.68 C, 0.32 T	N/A	0.76 C, 0.24 T	N/A	rs15775
Exon 6	c.513G→A (p.Q171Q)	0	0	0	0	1	0	0	N/A	
Exon 7	c.763G→A (p.D255N)	N/A	N/A	0	N/A	1	0	0	N/A	
Exon 8	c.816G→A (p.L272L)	N/A	N/A	0	N/A	0	N/A	1	N/A	
Exon 9	c.1177+77C→T	N/A	N/A	0.96 C, 0.04 T	N/A	0	N/A	0	N/A	rs858312
Exon 10	c.1380-12T→G	N/A	N/A	0	N/A	0	N/A	1	N/A	
Exon 10	c.1267C→T (p.H423Y)	N/A	N/A	0	N/A	0	N/A	1	N/A	
Exon 10	c.1353T→C (p.C451C)	N/A	N/A	0	N/A	0	N/A	1	N/A	
Exon 11	c.1414A→G (p.K472Q)	N/A	N/A	0	N/A	1	0	1	N/A	
Exon 11	c.1440A→G (p.K480K)	N/A	N/A	1	N/A	0	N/E	0	N/A	
Exon 12	c.1578T→C (p.V526V)	N/A	N/A	0	N/A	1	N/A	N/A	N/A	
3′ UTR	c.*7A→G	N/A	N/A	0	N/A	1	N/A	N/A	N/A	
3′ UTR	c.*23_35delinsTG	N/A	N/A	0	N/A	4	N/A	N/A	N/A	
Patients Analyzed										
		37	102	96	185	282	183 (Exon 6)	87	N/A	

Probands and unaffected controls were sequenced for changes in exons 1 through 12 of *KLHL7*. Abbreviations are as follows: RP, retinitis pigmentosa; adRP, autosomal-dominant retinitis pigmentosa; N.A., North American; U, university; N/A, no patients sequenced; N/E, not examined; UTR, untranslated region. Compound changes include one person with c.-235G→T and c.53A→G changes, one with c.1578T→C and c.*7A→G, two with c.53A→G and c.*23_35 delinsTG, and one with c.-235G→T, c.53A→G, and c.*23_35delinsTG. The c.1267C→T (p.H423Y) alteration was not observed as segregating with the disease and was therefore considered a non-disease-causing variant. North American controls numbering 166 individuals were examined for exons 7 and 11.

protein structure (data not shown). Examination of H bonding showed slightly varied bond lengths within the α1 and α2 helices of each corresponding mutant structure, including the formation of one additional H bond between residues 150 and 165 in the mutant S150N. Local tertiary structure inspection of α1 and α2 (Figure 4C, top left panel) shows that the introduction of mutant side chains appears to fill the space (i.e., cleft) between the two helices (Figure 4C, top right and lower panels).

Crystal structures of BTB-Kelch proteins are suggested to be similar to that of the Skp1-Cdc4 complex (PDB: 1nex).[20] α1 and α2 helices in the KLHL7 BACK-domain structure (based on PDB: 2eqxA) appear highly structurally similar (root mean square deviation [RMSD] = 0.84Å) to the C-terminal α5 and α6 helices of Skp1 (see PDB: 1nex) (Figure 4D, inset). Introduction of the three KLHL7 mutations did not show any gross structural effects. Notably, however, Skp1 and F box (see PDB: 1nex) proteins were suggested to associate by an "interdigitation of helices" that include Skp1 α5 and α6, giving rise to a "contiguous hydrophobic core" spanning the two proteins (Skp1 and F box).[22] We hypothesize that the side-chain space filling between α1 and α2, caused by KLHL7 mutations (S150N, A153V, and A153T), affects this "core" and the interaction or function of other domains of KLHL7 within the context of the overall protein.

Discussion

Retinal photoreceptors are highly metabolically active postmitotic neurons; it is estimated that 9 billion molecules of opsin are synthesized each second by approximately 120 million photoreceptors in the human retina.[23] Diurnal shedding and regeneration of membrane discs in the photoreceptors require stringent control of protein synthesis and transport.[24,25] Mutations in a variety of genes of varying function are associated with retinal degeneration. Several RP genes, such as *rhodopsin* (MIM 180380), *RP1* (MIM 603937), *CRX* (MIM 602225), and *NRL* (MIM 162080), are expressed primarily in the retina.[26–30] However, many other retinopathy-associated

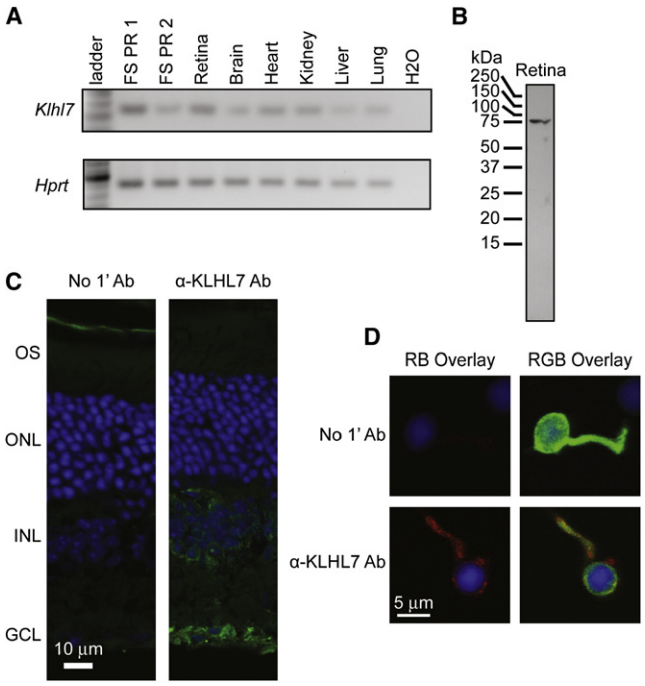

Figure 3. Expression Analysis and Protein Localization of KLHL7

(A) *Klhl7* RT-PCR product was observed in cDNA from various tissues (as indicated) and GFP-tagged flow-sorted rod photoreceptors (FS PR1 and FS PR2).

(B) Immunoblot analysis of KLHL7. A protein of approximately 75 kDa was observed in mouse retina with the use of an α-KLHL7 antibody. Predicted molecular mass of KLHL7 is ~65 kDa.

(C) Immunohistochemical characterization of KLHL7 protein. Mouse retina was incubated with secondary antibody only (left panel) or with α-KLHL7 (right panel). KLHL7 staining (green) is strong around the nuclei in the ganglion cell and the inner nuclear layer.

(D) Immunocytochemistry of a mouse rod photoreceptor. GFP-tagged photoreceptors were dissociated from Nrl-GFP mouse retina and incubated with an α-KLHL7 antibody. Weak KLHL7 staining (red) is detected around the nuclei (DAPI blue) of photoreceptors.

genes (e.g., *RPGR* [MIM 312610], *CEP290* [MIM 610142], *TOPORS* [MIM 609507], *PRPF3* [MIM 607301], *PRPF8* [MIM 607300], and *PRPF31* [MIM 606419]) are more broadly expressed.[31–36] Here, we identify a retinal-disease gene and suggest an additional cellular mechanism important for photoreceptor function and survival.

KLHL7 transcripts are widely expressed and detected even in mature oocytes and embryonic stem cells.[37] KLHL7 antibodies have been detected in Sjögren's syndrome and in cancer.[38,39] Although the physiological function of KLHL7 is not known, some clues may be derived from the published research on BTB family proteins that are associated with the ubiquitin-proteasome pathway of protein degradation.[21] BTB-Kelch family members, KLHL9 (MIM 611201) and KLHL13 (MIM 300655), are part of Cullin-based E3 ligase complexes involved in cell-cycle progression,[40] whereas KLHL12 is present in another Cullin-based E3 ligase complex, which targets the dopamine D4 receptor for ubiquitination.[41] The significance of protein-degradation pathways in neuronal development and function is underscored by the fact that protein aggregates are hallmarks of several neurodegenerative diseases.[42,43] Notably, mutations in another BTB-Kelch protein family member, *gigaxonin* (*GAN* [MIM 605379]), are responsible for giant axonal neuropathy.[44,45] Interestingly, the p.R138H mutation in gigaxonin[44] is at the same position in the BACK domain as p.S150 is in KLHL7, suggesting its critical role in mediating protein function.

Our discovery of three disease-causing KLHL7 mutations confined to the BACK domain and resulting specifically in dominant retinal degeneration suggests a key biological role for KLHL7 in cellular pathways. We postulate that KLHL7 functions in the ubiquitin-proteasome pathway and that mutations in its BACK domain affect the ability of KLHL7 to act as an intermediary or chaperone between an E3 ligase and its substrate. Failure to efficiently ubiquitinate a target substrate could then result in accumulation of the substrate(s) or aggregates, leading to cellular toxicity within the highly metabolically active photoreceptors. It is possible that mutations in other KLHL7 domains lead to a more severe phenotype or even lethality. Additional investigations are necessary for testing of this hypothesis.

In summary, the identification of *KLHL7* as an adRP gene introduces new facets for elucidating retinal biology and neurodegeneration.

Supplemental Data

Supplemental Data include one figure and two tables and can be found with this article online at http://www.ajhg.org/.

Acknowledgments

We sincerely acknowledge Abby Woodroffe for discussions; Rivka Rachel and Tiziana Cogliati for comments on the manuscript; and Mohammad Othman, Jessica Chang, Bob Fariss, Manessa Shaw, Ashley Garibaldi, Hema Karamchandani, and George Thomas for technical assistance. We thank Lucia Lawrence and Sharyn Ferrara for administrative support. This work was supported by NEI intramural funds and grants from the NIH, The Foundation Fighting Blindness, Harold F. Falls and Paul R. Lichter Professorships, Research to Prevent Blindness, the Elmer and Sylvia Sramek Foundation, the European Union (GENORET), The British Retinitis Pigmentosa Society (UK), The NIHR Biomedical Research Centre for Ophthalmology (UK), and the Swedish Medical Research Council.

Received: March 31, 2009
Revised: May 19, 2009
Accepted: May 20, 2009
Published online: June 11, 2009

Web Resources

The URLs for data presented herein are as follows:

DeepView (v4.0.1), http://www.expasy.org/spdbv/
Entrez, http://www.ncbi.nlm.nih.gov

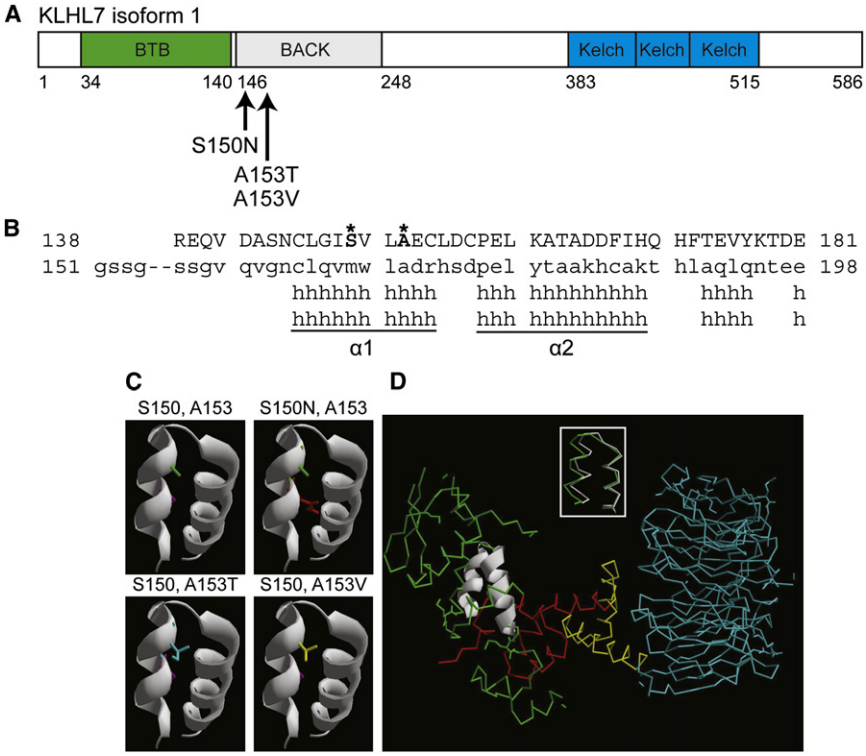

Figure 4. KLHL7 Protein Structure and Analysis

(A) Schematic of KLHL7 isoform 1. Mutations, reported here, are indicated.

(B) Protein alignment of the KLHL7 BACK domain to Kbtbd4. Mutant residues S150 and A153 are shown in bold and marked with an asterisk.

(C) Helical model of the KLHL7 BACK domain. S150 and A153 side chains are purple and green, respectively. Mutations 150N, 153T, and 153V are red, blue, and yellow, respectively. Each mutant side chain appears to occupy more space than the respective wild-type side chain in the cleft between two helices.

(D) Superimposition of α1 and α2 helices of the KLHL7 BACK domain on the Skp1 complex. The α1 and α2 helices of the KLHL7 BACK domain are structurally similar (RMSD = 0.84Å) to the α5 and α6 helices of Skp1 (inset). Green indicates Skp1. White is used to show an overlay of the BACK-domain α1 and α2 to α5 and α6 helices of Skp1. Red indicates the F box. Yellow indicates the helical linker. Blue indicates the WD40 domain. PDB:1nex.

Online Mendelian Inheritance in Man (OMIM), http://www.ncbi.nlm.nih.gov/Omim/
POV-Ray, http://povray.org
RetNet, http://www.sph.uth.tmc.edu/Retnet/
Swiss Model, http://swissmodel.expasy.org
WHAT IF, http://swift.cmbi.ru.nl

References

1. Hartong, D.T., Berson, E.L., and Dryja, T.P. (2006). Retinitis pigmentosa. Lancet *368*, 1795–1809.
2. Daiger, S.P., Bowne, S.J., and Sullivan, L.S. (2007). Perspective on genes and mutations causing retinitis pigmentosa. Arch. Ophthalmol. *125*, 151–158.
3. Sullivan, L.S., Bowne, S.J., Birch, D.G., Hughbanks-Wheaton, D., Heckenlively, J.R., Lewis, R.A., Garcia, C.A., Ruiz, R.S., Blanton, S.H., Northrup, H., et al. (2006). Prevalence of disease-causing mutations in families with autosomal dominant retinitis pigmentosa: A screen of known genes in 200 families. Invest. Ophthalmol. Vis. Sci. *47*, 3052–3064.
4. Sancho-Pelluz, J., Arango-Gonzalez, B., Kustermann, S., Romero, F.J., van Veen, T., Zrenner, E., Ekstrom, P., and Paquet-Durand, F. (2008). Photoreceptor cell death mechanisms in inherited retinal degeneration. Mol. Neurobiol. *38*, 253–269.
5. Ruschendorf, F., and Nurnberg, P. (2005). ALOHOMORA: A tool for linkage analysis using 10K SNP array data. Bioinformatics *21*, 2123–2125.
6. Abecasis, G.R., Cherny, S.S., Cookson, W.O., and Cardon, L.R. (2001). GRR: Graphical representation of relationship errors. Bioinformatics *17*, 742–743.
7. Wigginton, J.E., and Abecasis, G.R. (2005). PEDSTATS: Descriptive statistics, graphics and quality assessment for gene mapping data. Bioinformatics *21*, 3445–3447.
8. Mukhopadhyay, N., Almasy, L., Schroeder, M., Mulvihill, W.P., and Weeks, D.E. (2005). Mega2: Data-handling for facilitating genetic linkage and association analyses. Bioinformatics *21*, 2556–2557.
9. Abecasis, G.R., Cherny, S.S., Cookson, W.O., and Cardon, L.R. (2002). Merlin–rapid analysis of dense genetic maps using sparse gene flow trees. Nat. Genet. *30*, 97–101.
10. Friedman, J.S., Chang, B., Kannabiran, C., Chakarova, C., Singh, H.P., Jalali, S., Hawes, N.L., Branham, K., Othman, M., Filippova, E., et al. (2006). Premature truncation of a novel protein, RD3, exhibiting subnuclear localization is associated with retinal degeneration. Am. J. Hum. Genet. *79*, 1059–1070.
11. Akimoto, M., Cheng, H., Zhu, D., Brzezinski, J.A., Khanna, R., Filippova, E., Oh, E.C., Jing, Y., Linares, J.L., Brooks, M., et al. (2006). Targeting of GFP to newborn rods by Nrl promoter and temporal expression profiling of flow-sorted photoreceptors. Proc. Natl. Acad. Sci. USA *103*, 3890–3895.
12. Guex, N., and Peitsch, M.C. (1997). SWISS-MODEL and the Swiss-PdbViewer: An environment for comparative protein modeling. Electrophoresis *18*, 2714–2723.
13. Schwede, T., Kopp, J., Guex, N., and Peitsch, M.C. (2003). SWISS-MODEL: An automated protein homology-modeling server. Nucleic Acids Res. *31*, 3381–3385.
14. Kopp, J., and Schwede, T. (2004). The SWISS-MODEL Repository of annotated three-dimensional protein structure homology models. Nucleic Acids Res. *32*, D230–D234.
15. Arnold, K., Bordoli, L., Kopp, J., and Schwede, T. (2006). The SWISS-MODEL workspace: A web-based environment for protein structure homology modelling. Bioinformatics *22*, 195–201.
16. Vriend, G. (1990). WHAT IF: A molecular modeling and drug design program. J Mol Graph *8*, 52–56.

17. Andreasson, S. (1991). Electroretinographic studies of families with dominant retinitis pigmentosa. Acta Ophthalmol. (Copenh.) *69*, 162–168.
18. Inglehearn, C.F., Keen, T.J., al-Maghtheh, M., Gregory, C.Y., Jay, M.R., Moore, A.T., Bird, A.C., and Bhattacharya, S.S. (1994). Further refinement of the location for autosomal dominant retinitis pigmentosa on chromosome 7p (RP9). Am. J. Hum. Genet. *54*, 675–680.
19. Kremer, H., Pinckers, A., van den Helm, B., Deutman, A.F., Ropers, H.H., and Mariman, E.C. (1994). Localization of the gene for dominant cystoid macular dystrophy on chromosome 7p. Hum. Mol. Genet. *3*, 299–302.
20. Stogios, P.J., and Prive, G.G. (2004). The BACK domain in BTB-kelch proteins. Trends Biochem. Sci. *29*, 634–637.
21. Perez-Torrado, R., Yamada, D., and Defossez, P.A. (2006). Born to bind: The BTB protein-protein interaction domain. Bioessays *28*, 1194–1202.
22. Orlicky, S., Tang, X., Willems, A., Tyers, M., and Sicheri, F. (2003). Structural basis for phosphodependent substrate selection and orientation by the SCFCdc4 ubiquitin ligase. Cell *112*, 243–256.
23. Williams, D.S. (2002). Transport to the photoreceptor outer segment by myosin VIIa and kinesin II. Vision Res. *42*, 455–462.
24. Tan, E., Wang, Q., Quiambao, A.B., Xu, X., Qtaishat, N.M., Peachey, N.S., Lem, J., Fliesler, S.J., Pepperberg, D.R., Naash, M.I., et al. (2001). The relationship between opsin overexpression and photoreceptor degeneration. Invest. Ophthalmol. Vis. Sci. *42*, 589–600.
25. Lem, J., Krasnoperova, N.V., Calvert, P.D., Kosaras, B., Cameron, D.A., Nicolo, M., Makino, C.L., and Sidman, R.L. (1999). Morphological, physiological, and biochemical changes in rhodopsin knockout mice. Proc. Natl. Acad. Sci. USA *96*, 736–741.
26. Farrar, G.J., Kenna, P., Redmond, R., Shiels, D., McWilliam, P., Humphries, M.M., Sharp, E.M., Jordan, S., Kumar-Singh, R., and Humphries, P. (1991). Autosomal dominant retinitis pigmentosa: A mutation in codon 178 of the rhodopsin gene in two families of Celtic origin. Genomics *11*, 1170–1171.
27. Dryja, T.P., McGee, T.L., Reichel, E., Hahn, L.B., Cowley, G.S., Yandell, D.W., Sandberg, M.A., and Berson, E.L. (1990). A point mutation of the rhodopsin gene in one form of retinitis pigmentosa. Nature *343*, 364–366.
28. Pierce, E.A., Quinn, T., Meehan, T., McGee, T.L., Berson, E.L., and Dryja, T.P. (1999). Mutations in a gene encoding a new oxygen-regulated photoreceptor protein cause dominant retinitis pigmentosa. Nat. Genet. *22*, 248–254.
29. Freund, C.L., Gregory-Evans, C.Y., Furukawa, T., Papaioannou, M., Looser, J., Ploder, L., Bellingham, J., Ng, D., Herbrick, J.A., Duncan, A., et al. (1997). Cone-rod dystrophy due to mutations in a novel photoreceptor-specific homeobox gene (CRX) essential for maintenance of the photoreceptor. Cell *91*, 543–553.
30. Bessant, D.A., Payne, A.M., Mitton, K.P., Wang, Q.L., Swain, P.K., Plant, C., Bird, A.C., Zack, D.J., Swaroop, A., and Bhattacharya, S.S. (1999). A mutation in NRL is associated with autosomal dominant retinitis pigmentosa. Nat. Genet. *21*, 355–356.
31. Meindl, A., Dry, K., Herrmann, K., Manson, F., Ciccodicola, A., Edgar, A., Carvalho, M.R., Achatz, H., Hellebrand, H., Lennon, A., et al. (1996). A gene (RPGR) with homology to the RCC1 guanine nucleotide exchange factor is mutated in X-linked retinitis pigmentosa (RP3). Nat. Genet. *13*, 35–42.
32. den Hollander, A.I., Koenekoop, R.K., Yzer, S., Lopez, I., Arends, M.L., Voesenek, K.E., Zonneveld, M.N., Strom, T.M., Meitinger, T., Brunner, H.G., et al. (2006). Mutations in the CEP290 (NPHP6) gene are a frequent cause of Leber congenital amaurosis. Am. J. Hum. Genet. *79*, 556–561.
33. Chakarova, C.F., Papaioannou, M.G., Khanna, H., Lopez, I., Waseem, N., Shah, A., Theis, T., Friedman, J., Maubaret, C., Bujakowska, K., et al. (2007). Mutations in TOPORS cause autosomal dominant retinitis pigmentosa with perivascular retinal pigment epithelium atrophy. Am. J. Hum. Genet. *81*, 1098–1103.
34. Chakarova, C.F., Hims, M.M., Bolz, H., Abu-Safieh, L., Patel, R.J., Papaioannou, M.G., Inglehearn, C.F., Keen, T.J., Willis, C., Moore, A.T., et al. (2002). Mutations in HPRP3, a third member of pre-mRNA splicing factor genes, implicated in autosomal dominant retinitis pigmentosa. Hum. Mol. Genet. *11*, 87–92.
35. McKie, A.B., McHale, J.C., Keen, T.J., Tarttelin, E.E., Goliath, R., van Lith-Verhoeven, J.J., Greenberg, J., Ramesar, R.S., Hoyng, C.B., Cremers, F.P., et al. (2001). Mutations in the pre-mRNA splicing factor gene PRPC8 in autosomal dominant retinitis pigmentosa (RP13). Hum. Mol. Genet. *10*, 1555–1562.
36. Vithana, E.N., Abu-Safieh, L., Allen, M.J., Carey, A., Papaioannou, M., Chakarova, C., Al-Maghtheh, M., Ebenezer, N.D., Willis, C., Moore, A.T., et al. (2001). A human homolog of yeast pre-mRNA splicing gene, PRP31, underlies autosomal dominant retinitis pigmentosa on chromosome 19q13.4 (RP11). Mol. Cell *8*, 375–381.
37. Assou, S., Cerecedo, D., Tondeur, S., Pantesco, V., Hovatta, O., Klein, B., Hamamah, S., and De Vos, J. (2009). A gene expression signature shared by human mature oocytes and embryonic stem cells. BMC Genomics *10*, 10.
38. Uchida, K., Akita, Y., Matsuo, K., Fujiwara, S., Nakagawa, A., Kazaoka, Y., Hachiya, H., Naganawa, Y., Oh-Iwa, I., Ohura, K., et al. (2005). Identification of specific autoantigens in Sjogren's syndrome by SEREX. Immunology *116*, 53–63.
39. Bredholt, G., Storstein, A., Haugen, M., Krossnes, B.K., Husebye, E., Knappskog, P., and Vedeler, C.A. (2006). Detection of autoantibodies to the BTB-kelch protein KLHL7 in cancer sera. Scand. J. Immunol. *64*, 325–335.
40. Sumara, I., Maerki, S., and Peter, M. (2008). E3 ubiquitin ligases and mitosis: Embracing the complexity. Trends Cell Biol. *18*, 84–94.
41. Rondou, P., Haegeman, G., Vanhoenacker, P., and Van Craenenbroeck, K. (2008). BTB Protein KLHL12 targets the dopamine D4 receptor for ubiquitination by a Cul3-based E3 ligase. J. Biol. Chem. *283*, 11083–11096.
42. Rubinsztein, D.C. (2006). The roles of intracellular protein-degradation pathways in neurodegeneration. Nature *443*, 780–786.
43. Tai, H.C., and Schuman, E.M. (2008). Ubiquitin, the proteasome and protein degradation in neuronal function and dysfunction. Nature reviews *9*, 826–838.
44. Bomont, P., Cavalier, L., Blondeau, F., Ben Hamida, C., Belal, S., Tazir, M., Demir, E., Topaloglu, H., Korinthenberg, R., Tuysuz, B., et al. (2000). The gene encoding gigaxonin, a new member of the cytoskeletal BTB/kelch repeat family, is mutated in giant axonal neuropathy. Nat. Genet. *26*, 370–374.
45. Yang, Y., Allen, E., Ding, J., and Wang, W. (2007). Giant axonal neuropathy. Cell. Mol. Life Sci. *64*, 601–609.